4. Natural Demodulation of Two-Dimensional Fringe Patterns: Stationary Phase Analysis of the Spiral Phase Quadrature Transform

He is anxious for me to make use of his brain, ha, ha! – not, as you might suppose, as a floating specimen in one of my jam jars, ha, ha, ha! But in its functional capacity as a vortex of dazzling thought

Dr Prunesqallor (in Mervyn Peake's Titus Groan)

4.1 Introduction

In the preceding chapters novel techniques for demodulating quite specific one and two-dimensional wavefields have been investigated. In this chapter the extension to more general two-dimensional patterns is considered. The two-dimensional patterns considered can be classified as fringe patterns. The working definition of such patterns is a pattern with fringe spacing and fringe orientation defined (almost) everywhere. Patterns which fall into this category include optical interferograms, holograms, ripples in sand dunes and human fingerprints. Such patterns are also know as ridge systems[1] and oriented patterns.[2, 3] The development of a general method for isotropically demodulating such patterns will not be presented in this thesis

because it is the combined work of a group. However the task of finding a mathematical proof of the underlying transform is undertaken in this chapter.

4.2 A quite remarkable transform

Recently Larkin, Bone, and Oldfield[4] have proposed a "revolutionary" spiral-phase quadrature transform for two-dimensional fringe patterns. The transform was developed for the isotropic demodulation of fingerprints and other complex 2-D patterns by these researchers at Canon Information Systems Research Australia. Such a transform was previously considered impossible by many researchers. The proposed transform has many properties in common with an idealised 2-D Hilbert transform, and opens up many applications in image and pattern analysis. The history and background of that transform are covered in the initial publication by Larkin et al. In this chapter a mathematical proof of the central property of the spiral phase quadrature transform (or *vortex transform* for short) is developed. The proof is developed through the method of stationary phase applied to a two-dimensional fringe pattern of quite general form. As far as I am aware this powerful method has not been successfully applied to the demodulation and analysis of fringe patterns before. Stationary phase methods are however familiar in the closely related field of computer generated holograms.[5, 6]

This chapter is organised as follows. In section 4.3 I consider the definition of a two-dimensional fringe pattern and some methods available for demodulation. In section 4.4 I use the method of stationary phase to estimate the Fourier transform of a complex fringe pattern and then introduce the orientational phase factor and its spectral twin the spiral phase factor. In section 4.5 it is shown that a real fringe

pattern can be constructed from two complex conjugate patterns and that a quadrature relation can be established using the spiral phase factor. Section 4.6 reviews the heuristic development of the spiral phase quadrature transform. Section 4.7 considers an alternative stationary phase expansion that indicates how the spiral phase quadrature relation deviates from the ideal. The conclusion in section 4.8 is followed by discussion of connections with preceding work in section 4.9. An appendix on the practical aspects of orientation estimation is included for completeness.

4.3 Two Dimensional Fringe Patterns

For simplicity we shall consider a general fringe pattern intensity function $f(x,y)$ of the form

$$f(x,y) = b(x,y)\cos\psi(x,y) = \frac{b(x,y)}{2}\left\{\exp\left[i\psi(x,y)\right] + \exp\left[-i\psi(x,y)\right]\right\} \qquad (4.1)$$

where the conventional offset (or "DC") term has been removed for simplicity.[7] The objective of fringe pattern analysis is to extract both the amplitude and phase modulation terms, $b(x,y)$ and $\phi(x,y)$ respectively. The analysis process is better described in general as two-dimensional demodulation. One way to demodulate is by estimation of the fringe quadrature component $\hat{f}(x,y)$:

$$\hat{f}(x,y) = -b(x,y)\sin\psi(x,y) = -\frac{b(x,y)}{2i}\left\{\exp\left[i\psi(x,y)\right] - \exp\left[-i\psi(x,y)\right]\right\}. \qquad (4.2)$$

In one dimension it is well known that this quadrature process can be approximated by the Hilbert transform (the error in the approximation is related to how well the function fits certain bandlimit constraints[8]). A significant body of detailed work exists on this subject and it is covered in a number of standard texts as well as being the basis of the "Fourier Transform Method" (or FTM) in fringe analysis.[9] In two (or more) dimensions the problem requires the definition of a Hilbert transform (HT) analogous to the one-dimensional case.[10] In most cases this has led to simple extensions based upon separable products of the 1-D HT. Readers interested in previous attempts to extend the HT beyond 1-D are advised to consult the attachments to this thesis.[4] The starting point for the idea of a 2-D Hilbert transform is based upon a spiral phase "signum function". It is worth noting at this point that iterative methods for 2-D demodulation can give excellent results for suitably smooth fringe patterns, although the computational requirements are significant.[11] From the image processing perspective it is often preferable to have an algorithm which computes the results efficiently via a direct method, if such a method exists. The spiral phase quadrature transform is one such direct method.

4.4 Stationary Phase Expansion of a Complex Pattern *p(x,y)*

It is not the objective of this work to give a formal justification of the method of stationary phase. A number of clear, detailed and rigorous accounts are available. A book by Bleistein and Handlesman contains details of stationary phase method for multiple dimension integrals of Fourier type.[12] Their approach is followed by initially considering an integral with a complex exponential kernel $p(x,y)$ (analogous to the

analytic signal in one dimension[13, 14]) and then later separating the real and imaginary parts corresponding to the two quadrature functions

$$p(x,y) = f(x,y) - i\hat{f}(x,y) = b(x,y)\exp\left[i\psi(x,y)\right]. \tag{4.3}$$

The 2-D Fourier transform is defined as follows:

$$P(u,v) = \int_{-\infty}^{+\infty}\int_{-\infty}^{+\infty} p(x,y)\exp\left[2\pi i(ux+vy)\right]dxdy. \tag{4.4}$$

This can be written more compactly as

$$P(u,v) = \int_{-\infty}^{+\infty}\int_{-\infty}^{+\infty} b(x,y)\exp\left[i\Psi(u,v,x,y)\right]dxdy. \tag{4.5}$$

The total phase function being $\Psi(u,v,x,y) = \psi(x,y) - 2\pi(ux+vy)$. Now parameterise the transforms with a factor k that represents a fringe pattern with increasingly close fringes, but unchanged envelope:

$$P_k(u,v) = \int_{-\infty}^{+\infty}\int_{-\infty}^{+\infty} b(x,y)\exp\left[ik\Psi(u,v,x,y)\right]dxdy. \tag{4.6}$$

If a particular location in frequency space (u,v) is considered, then the above equation corresponds to the integral forms considered by Bleistein (page 340). In this particular case functions are further restricted to allow a simple derivation:

- $b(x,y)$ is a real function, continuous and infinitely differentiable,
- $\Psi(x,y)$ is also a real function, continuous and infinitely differentiable.

Figure 4.1(a) shows an example of a fringe pattern which satisfies the above restrictions. The underlying phase function $\psi(x,y)$ for the depicted fringe pattern is shown in figure 4.1(b). The above restrictions allow us to ignore critical points of the second and third kinds, which would otherwise occur at the edges and corners of the support boundary.

Now the method of stationary phase can be applied directly to equation (4.6) and – following Stamnes[15] (page 138) - the result is the sum of contributions from all the critical points:

$$P_k(u_s,v_s) \sim \frac{2\pi}{k}\sum_{n=1}^{N}\frac{\sigma(x_n,y_n)}{\left|H(x_n,y_n)\right|^{1/2}}\exp\left[ik\Psi(x_n,y_n)\right]\left\{b(x_n,y_n)+\frac{i}{k}Q_2(x_n,y_n)\right\} \quad (4.7)$$

where the critical points are defined in 2-D by the phase gradient zeroes

$$\nabla\Psi(x,y)=0 \quad \Rightarrow \Psi_{1,0}(x,y)=\Psi_{0,1}(x,y)=0 \quad \text{at } x=x_n,\ y=y_n\,. \quad (4.8)$$

There is a magnitude term related to the Hessian[16], H, of the phase at each critical point, where

$$H(x_n,y_n)=\Psi_{2,0}(x_n,y_n)\Psi_{0,2}(x_n,y_n)-\Psi_{1,1}^2(x_n,y_n), \quad (4.9)$$

Figure 4.1(a).
A typical fringe pattern with smooth and differentiable amplitude and phase.

Figure 4.1(b).
Underlying phase function of the fringe pattern in figure 4.1(a). The greyscale representation has black for zero radians and white for 70 radians.

and the partial derivative of the phase is

$$\Psi_{l,m} = \frac{\partial^{l+m}\Psi}{\partial x^l \partial y^m}. \tag{4.10}$$

The factor σ is controlled by the shape of the stationary point

$$\sigma = \begin{cases} 1 & \text{if } H < 0 \\ i & \text{if } H > 0, \Psi_{2,0} > 0 \\ -i & \text{if } H > 0, \Psi_{2,0} < 0 \end{cases}. \tag{4.11}$$

Stamnes includes a second order term Q_2 related to products of various partial derivatives and the reciprocal of the Hessian

$$Q_2 \sim \frac{1}{H(x_n, y_n)}. \tag{4.12}$$

The first order analysis will ignore this term. It is assumed here that the stationary points (x_n, y_n) are all of lowest order. Higher order stationarity can be defined although the expressions become rather complex unless described recursively. Mathematically this assumption is expressed as

$$H(x_n, y_n) \neq 0. \tag{4.13}$$

In the case where the stationary points are not isolated the coefficients will be modified (Papoulis[17] gives a nice example where a line of points give a $k^{-1/2}$ rather than a k^{-1} asymptotic coefficient). Again such complications are ignored in the present analysis, as the main objective is show that the vortex operator is valid for many, if not all, possible fringe patterns. The actual locations of the (isolated) stationary points are related to particular spatial frequencies:

$$\left.\begin{aligned}\psi_{1,0}\left(x_n, y_n\right) &= 2\pi u_s \\ \psi_{0,1}\left(x_n, y_n\right) &= 2\pi v_s\end{aligned}\right\}. \tag{4.14}$$

A Taylor's series expansion around each stationary point gives:

$$\begin{aligned}&\psi\left(x_n + s, y_n + t\right) = \\ &\quad \psi_{0,0}\left(x_n, y_n\right) + \psi_{1,0}\left(x_n, y_n\right)s + \psi_{0,1}\left(x_n, y_n\right)t + \frac{\psi_{2,0}\left(x_n, y_n\right)s^2}{2} + \frac{\psi_{0,2}\left(x_n, y_n\right)t^2}{2} + \ldots\end{aligned} \tag{4.15}$$

so that

$$\Psi\left(x_n + s, y_n + t\right) = \psi_{0,0}\left(x_n, y_n\right) + \frac{\psi_{2,0}\left(x_n, y_n\right)s^2}{2} + \frac{\psi_{0,2}\left(x_n, y_n\right)t^2}{2} + \frac{\psi_{1,1}\left(x_n, y_n\right)st}{1} + \ldots \tag{4.16}$$

The contribution to the Fourier integral from any one stationary point $\left(x_n, y_n\right)$ is

$$P_k(u_s,v_s)_n \sim \frac{2\pi}{k}\frac{\sigma(x_n,y_n)}{\left|H(x_n,y_n)\right|^{1/2}}\exp\left[ik\psi(x_n,y_n)\right]b(x_n,y_n). \qquad (4.17)$$

Now consider another stationary phase expansion of the original fringe pattern, but this time with a slowly varying phase factor $\exp\left[i\beta(x,y)\right]$ applied to the amplitude modulation term $b(x,y)$. If the phase factor is suitably slowly varying and differentiable we can justify this (later the alternative of applying it to the phase modulation term is considered). Of particular interest is a phase factor that corresponds to the fringe orientation angle (orientation of steepest phase gradient):

$$\tan\beta(x,y)=\frac{\psi_{0,1}(x,y)}{\psi_{1,0}(x,y)},\quad 0\le\beta<2\pi. \qquad (4.18)$$

Figure 4.2 (a) shows the general definition of orientation angle from the phase gradient. Figure 4.2 (b) shows the corresponding case for a real fringe pattern. An orientation defined by equation (4.18) is unambiguous in the range 0° to 360° (modulo 2π), unlike the orientation of real fringe patterns where it is not possible to distinguish a fringe from a similar fringe rotated 180° (in other words the estimation is modulo π).

Figure 4.3(a) shows a greyscale plot of the orientational phase (modulo π) for the fringe pattern in figure 4.1(a). Figure 4.3(b) shows a greyscale plot of the orientational phase (modulo 2π) for the phase function shown in figure 4.1(b).

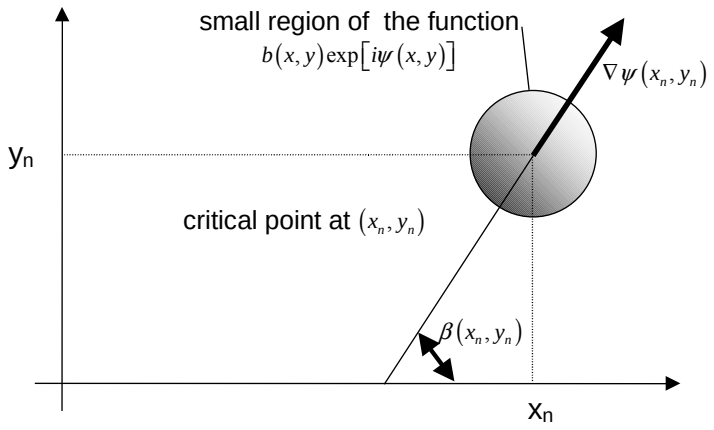

Figure 4.2 (a).
The definition of orientation angle from the phase gradient.

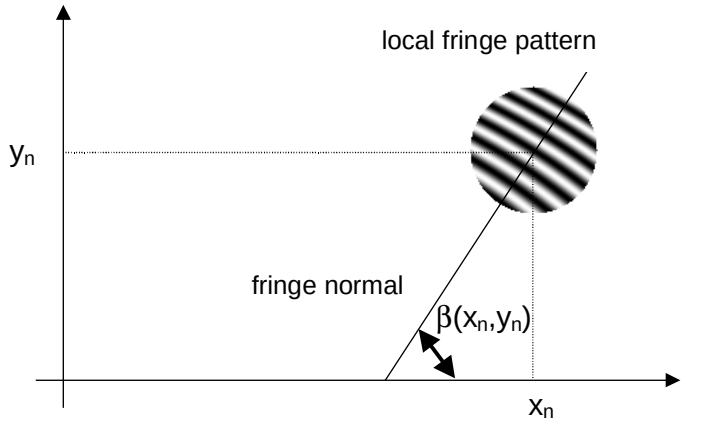

Figure 4.2 (b)
The definition of orientation angle from fringe angle.

Readers interested in implementation details are referred to appendix A where certain practical aspects of estimating the fringe orientation angle are discussed.

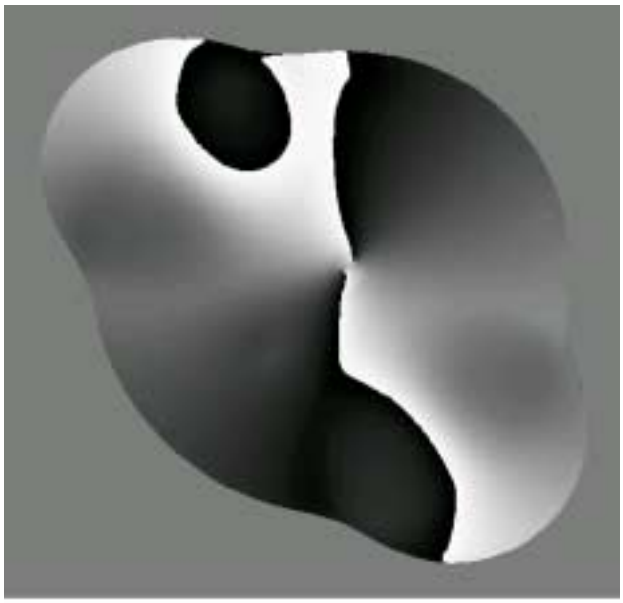

Figure 4.3(a).
Simple square root of orientation phase map (modulo π).

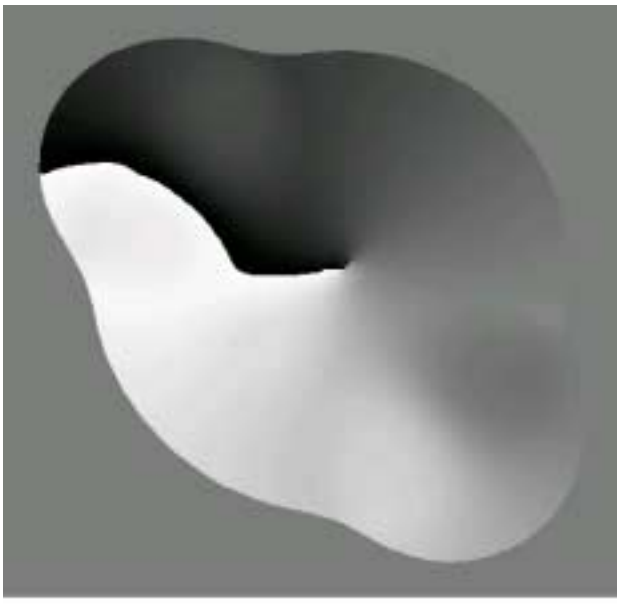

Figure 4.3(b).
Unwrapped orientation phase map (modulo 2π). Greyscale encoding means black represents $-\pi$ and white represents $+\pi$.

The Fourier transform of the modified fringe pattern becomes

$$\tilde{P}_k(u,v) = \int_{-\infty}^{+\infty}\int_{-\infty}^{+\infty} \tilde{b}(x,y)\exp\left[ik\Psi(u,v,x,y)\right]dxdy \tag{4.19}$$

where the new amplitude, $\tilde{b}$, is given by

$$\tilde{b}(x_n,y_n) = b(x_n,y_n)\exp\left[i\beta(x_n,y_n)\right] = b(x_n,y_n)\frac{\psi_{1,0}(x_n,y_n)+i\psi_{0,1}(x_n,y_n)}{\sqrt{\psi_{1,0}^2(x_n,y_n)+\psi_{0,1}^2(x_n,y_n)}}. \tag{4.20}$$

But, as shown in equation (4.14), the first order phase derivatives at isolated stationary points correspond directly to a specific frequency (u_s,v_s)

$$\tilde{b}(x_n,y_n) = b(x_n,y_n)\frac{u_s+iv_s}{\sqrt{u_s^2+v_s^2}}. \tag{4.21}$$

Polar frequency coordinates (q,ϕ) can be defined

$$\left.\begin{aligned} u &= q\cos\phi(u,v)\\ v &= q\sin\phi(u,v)\end{aligned}\right\} \tag{4.22}$$

hence

$$\tilde{b}(x_n,y_n) = b(x_n,y_n)\frac{u+iv}{q} = b(x_n,y_n)\exp\left[i\phi_s(u_s,v_s)\right]. \tag{4.23}$$

The resulting asymptotic approximation is

$$\tilde{P}_k(u_s,v_s)_n \sim \frac{2\pi}{k}\frac{\sigma(x_n,y_n)}{\left|H(x_n,y_n)\right|^{1/2}}\exp\left[ik\psi(x_n,y_n)\right]b(x_n,y_n)\exp\left[i\phi(u_s,v_s)\right]. \tag{4.24}$$

In other words, multiplying a complex exponential pattern $p(x,y)$ in the space domain by an orientation phase factor $\exp\left[i\beta(x,y)\right]$ results in a Fourier transform that is unaltered except for a spiral phase factor $\exp\left[i\phi\right]$. The multiplicative phase factors are Fourier twins. Equation (4.24) is a key result of this chapter, and is a specific instance of the more general result to be demonstrated. The result also applies directly to the complex conjugate pattern $p^*(x,y)$, which has a reversed orientational phase factor $\exp\left[-i\beta(x,y)\right]$ but yields the same Fourier phase factor $\exp\left[i\phi\right]$ because the corresponding frequency components rotate 180°. The result for the complex conjugate pattern with the original orientation phase factor $\exp\left[i\beta(x,y)\right]$ is given by

$$g(x,y) = p^*(x,y) = b(x,y)\exp\left[-i\psi(x,y)\right]. \tag{4.25}$$

The rotated components are

$$G_k(-u_s,-v_s)_n \sim \frac{2\pi}{k}\frac{\sigma(x_n,y_n)}{\left|H(x_n,y_n)\right|^{1/2}}\exp\left[-ik\psi(x_n,y_n)\right]b(x_n,y_n). \tag{4.26}$$

Modifying the conjugate pattern by the orientation phase factor

$$\tilde{g}(x,y) = p^*(x,y)\exp\left[i\beta(x,y)\right]. \tag{4.27}$$

Finally its Fourier components are

$$\tilde{G}_k(-u_s,-v_s)_n \sim \frac{2\pi}{k}\frac{\sigma(x_n,y_n)}{\left|H(x_n,y_n)\right|^{1/2}}\exp\left[-ik\psi(x_n,y_n)\right]b(x_n,y_n)\left(\frac{u_s+iv_s}{\sqrt{u_s^2+v_s^2}}\right). \tag{4.28}$$

This can be rewritten with the local spiral phase factor and a significant sign reversal

$$\tilde{G}_k(-u_s,-v_s)_n \sim -\frac{2\pi}{k}\frac{\sigma(x_n,y_n)}{\left|H(x_n,y_n)\right|^{1/2}}\exp\left[-ik\psi(x_n,y_n)\right]b(x_n,y_n)\exp\left[i\phi(-u_s,-v_s)\right]. \tag{4.29}$$

4.5 Stationary Phase Expansion of a Real Fringe Pattern *f(x,y)*

The result for the complex fringe pattern has been derived; now consider the original real fringe pattern. The cosine term consists of positive and negative phase components. The general relation between the FT of a function and the FT of the complex conjugate of a function can be written

$$p(x,y) \rightleftharpoons P(u,v) \Rightarrow p^*(x,y) \rightleftharpoons P^*(-u,-v). \tag{4.30}$$

where the FT relation is represented by the symbol $\rightleftharpoons$. Clearly $F(u,v)$ is Hermitian, because $f(x,y)$ is real, and

$$F(u,v) = \frac{P(u,v) + P^*(-u,-v)}{2} = F^*(-u,-v). \tag{4.31}$$

So the complete FT is composed of two parts, the second of which is obtained by rotating the first by 180° and then conjugating it. In terms of the original stationary phase approximation to $P(u,v)$: each critical point (x_n, y_n) contributes a component at frequency (u_s, v_s) and a complex conjugated component at frequency $(-u_s, -v_s)$. In general the function $P(u,v)$ may occupy a large region of the frequency domain, and hence $P^*(-u,-v)$ is quite likely to overlap $P(u,v)$ significantly. This overlap is the source of the difficulty Fourier based methods have in analysing closed fringe patterns. Masks simply cannot separate overlapping components in the Fourier domain. Something more subtle than masking is required.

Consider the real fringe pattern modified by the orientational phase factor

$$\tilde{f}(x,y) = \tilde{b}(x,y)\cos\psi(x,y)$$

$$\tilde{f}(x,y) = \frac{b(x,y)}{2}\exp\left[i\beta(x,y)\right]\left\{\exp\left[i\psi(x,y)\right] + \exp\left[-i\psi(x,y)\right]\right\}. \tag{4.32}$$

The orientational phase factor here is the modulo 2π form (see appendix) simultaneously applied to both positive and negative exponential components of the fringe pattern. Applying the FT and considering only those components at the two

diametrical frequencies (u_s, v_s) and $(-u_s, -v_s)$ due to the stationary phase critical points at (x_n, y_n) previously defined (equations (4.24) and (4.29)), gives

$$2\tilde{F}_{s,n}(u,v) = \tilde{P}_k(u_s, v_s)_n \, \delta(u-u_s, v-v_s) + \tilde{G}_k(-u_s, -v_s)_n \, \delta(u+u_s, v+v_s). \tag{4.33}$$

Expanding terms gives

$$2\tilde{F}_{s,n}(u,v) \sim \frac{2\pi}{k} \frac{\sigma(x_n, y_n)}{|H(x_n, y_n)|^{1/2}} b(x_n, y_n) \exp[i\phi(u_s, v_s)] \times$$
$$\{\exp[ik\psi(x_n, y_n)]\delta(u-u_s, v-v_s) - \exp[-ik\psi(x_n, y_n)]\delta(u+u_s, v+v_s)\}. \tag{4.34}$$

The above equation is recognisable as the Fourier transform of a quadrature fringe pattern multiplied by a spiral phase factor. In particular for a real fringe pattern $w(x, y)$ defined by

$$w(x, y) = b(x, y) \sin \psi(x, y) \tag{4.35}$$

it can be shown, using the preceding methods, that the Fourier transform components due to the stationary point (x_n, y_n) are

$$2iW_{s,n}(u,v) \sim \frac{2\pi}{k}\frac{\sigma(x_n,y_n)}{\left|H(x_n,y_n)\right|^{1/2}} b(x_n,y_n)\times$$
$$\left\{\exp\left[ik\psi(x_n,y_n)\right]\delta(u-u_s,v-v_s) - \exp\left[-ik\psi(x_n,y_n)\right]\delta(u+u_s,v+v_s)\right\}. \tag{4.36}$$

Combining equations (4.34) and (4.36) results in

$$2\tilde{F}_{s,n}(u,v) = 2iW_{s,n}(u,v)\exp\left[i\phi(u_s,v_s)\right]. \tag{4.37}$$

In other words, applying the orientational phase function to the real fringe pattern f corresponds to a multiplication by a spiral function in the Fourier domain, where the multiplication applies to the FT of the fringe quadrature function. The converse is also true (within the stationary phase approximation). The spiral phase can be considered to apply over the full Fourier plane, not just at the two diametrical frequencies, without loss of generality. The complete Fourier transform expression is to be formed by summing (integrating) the contributions from all critical points because the process is additive (all points with the same β result in Fourier components at polar angle ϕ)

The overall process in equation (4.37) can be summarised in operator notation with $\mathrm{F}\{\ \}$ and $\mathrm{F}^{-1}\{\ \}$ representing the forward and inverse Fourier transform operators respectively

$$\mathrm{F}\left\{\exp(-i\beta)b\cos\psi\right\} \sim \exp(i\phi)\mathrm{F}\left\{ib\sin\psi\right\}. \tag{4.38}$$

The proposed spiral phase transform can be succinctly expressed by

$$\mathrm{F}^{-1}\left\{\exp(i\phi)\,\mathrm{F}\{b\sin\psi\}\right\} \sim -i\exp(i\beta)\,b\cos\psi\,. \tag{4.39}$$

The result is to be considered asymptotically correct in the sense of a first order stationary phase expansion of a function containing only critical points of the first kind. Alternatively, starting with a quadrature fringe pattern yields the following relations (replacing $\psi = \psi' + \pi/2$)

$$\mathrm{F}^{-1}\left\{\exp(i\phi)\,\mathrm{F}\{b\cos\psi'\}\right\} \sim +i\exp(i\beta)\,b\sin\psi'\,. \tag{4.40}$$

Finally, the transform which I call the "spiral phase quadrature transform" or vortex transform for short results:

$$b\sin\psi \sim -i\exp(-i\beta)\,\mathrm{F}^{-1}\left\{\exp(i\phi)\,\mathrm{F}\{b\cos\psi\}\right\}. \tag{4.41}$$

Equation (4.41) represents a direct and efficient method for estimating the quadrature component of a quite general 2-D fringe pattern, and hence a natural method of 2-D demodulation. The transform can be performed optically with just two phase-only holograms, in a manner reminiscent of a general coordinate transformation using multiple holographic elements.[6]

4.6 Heuristic development of the Spiral Phase Quadrature Transform

The preceding derivations have been, by necessity, rather circuitous and non-intuitive. The stationary phase theory was developed quite some time after the vortex transform was discovered experimentally. In turn, the experimental discovery was prompted by a number of heuristic arguments for the essential features of a 2-D quadrature transform outlined in the initial exposition.[4]

The essential heuristic reasoning follows. Figure 4.2(b) shows that each region in the interferogram has a well defined fringe orientation (β_0), and spacing. The stationary phase method allows components which contribute to the FT from each such region (at a pair of diametrically opposed frequencies) to be evaluated. If the FT is multiplied by a pure spiral phase factor, then the polarity of these components at opposite frequencies is flipped (because the phase spiral is an odd function) while each maintains the fixed local phase factor $\exp(i\beta_0)$. Calculating the inverse FT now gives a quadrature function with an orientational phase factor $\exp(i\beta_0)$, which can be neutralised if the local fringe orientation can be estimated (or is known). Note that the orientation should be modulo 2π because it is originally defined by the gradient of the phase derivative without any sign related ambiguities. In essence, the stationary phase method allows small region of the complex "analytic" image[13] underlying the interferogram to be isolated when the number of fringes in that region tends to infinity. This results in the relative curvature of the fringes diminishing (here the relative curvature is defined as the fringe spacing divided by the radius of curvature) so that the fringes are effectively straight and only contribute to a single frequency component determined by the phase gradient.

4.7 Deviations From the Ideal Quadrature Transform

In section 4.4 the stationary phase expansion of an integral with an orientational phase factor $\exp(i\beta)$ applied to the amplitude function was considered. The justification for this is that the factor is slowly varying. If however the factor is considered to be of significant variation, then it should be included in the rapidly varying phase part. This approach is appropriate for patterns with widely spaced fringes or tightly curved fringes. In this section the implications of such modifications are investigated

The integral to consider is similar to that in section 3, equation (4.6)

$$\breve{P}_k(u,v) = \int_{-\infty}^{+\infty}\int_{-\infty}^{+\infty} b(x,y)\exp\left\{k\left[i\Psi(u,v,x,y) - i\beta(x,y)\right]\right\}dxdy\,. \tag{4.42}$$

It is worth pausing to consider what this integral means physically as the parameter k tends to infinity. In section 4.4 the orientational phase is independent of k and the limit represents a single spiral acting on a fringe pattern with very finely spaced fringes. In this section the orientational phase increases as the fringe spacing decreases. This means that the spiral component maintains the same strength relative to the fringe pattern phase so that relative error effects are maintained as k tends to infinity. The stationary phase expansion is thus

$$\breve{P}_k(\breve{u}_s,\breve{v}_s)_n \sim \frac{2\pi}{k}\frac{\breve{\sigma}(\breve{x}_n,\breve{y}_n)}{\left|\breve{H}(\breve{x}_n,\breve{y}_n)\right|^{1/2}}\exp\left[ik\breve{\Psi}(\breve{x}_n,\breve{y}_n)\right]b(\breve{x}_n,\breve{y}_n)\,. \tag{4.43}$$

The essential change occurs in the stationary point conditions because the orientational phase has a non-zero gradient that induces a shift in the overall phase gradient. The overall phase function is now

$$\breve{\Psi}(u,v,x,y) = \psi(x,y) - 2\pi(ux+vy) - \beta(x,y). \tag{4.44}$$

The stationary point conditions are again determined by the null gradient

$$\nabla\breve{\Psi}(\breve{u}_s,\breve{v}_s,\breve{x}_n,\breve{y}_n) = 0. \tag{4.45}$$

The shift in the frequencies is more explicitly shown by

$$\left.\begin{aligned}\psi_{1,0}(\breve{x}_n,\breve{y}_n) - \beta_{1,0}(\breve{x}_n,\breve{y}_n) &= 2\pi\breve{u}_s = 2\pi(u_s - \Delta u_s)\\ \psi_{0,1}(\breve{x}_n,\breve{y}_n) - \beta_{0,1}(\breve{x}_n,\breve{y}_n) &= 2\pi\breve{v}_s = 2\pi(v_s - \Delta v_s)\end{aligned}\right\}. \tag{4.46}$$

Using the original definition of the fringe orientation as the direction of the initial phase gradient gives

$$\left.\begin{aligned}2\pi\Delta u_s = \beta_{1,0} &= \frac{\psi_{1,0}\psi_{1,1} - \psi_{0,1}\psi_{2,0}}{\psi_{1,0}^2 + \psi_{0,1}^2} = \frac{u_s\psi_{1,1} - v_s\psi_{2,0}}{q_s^2}\\ 2\pi\Delta v_s = \beta_{0,1} &= \frac{\psi_{1,0}\psi_{0,2} - \psi_{0,1}\psi_{1,1}}{\psi_{1,0}^2 + \psi_{0,1}^2} = \frac{u_s\psi_{0,2} - v_s\psi_{1,1}}{q_s^2}\end{aligned}\right\}. \tag{4.47}$$

This means that the frequency shift due to the orientational phase factor is exactly zero, if and only if $\beta_{0,1} = \beta_{1,0} = 0$. This can only occur if the Gaussian curvature or Hessian *H* of the underlying phase function is zero:

$$\psi_{2,0}\psi_{0,2} - \psi_{1,1}^2 = 0\,. \tag{4.48}$$

This is then a necessary, but not sufficient,[18] condition. In effect this means that frequency shifts due to the orientational phase will not occur in regions where the fringes are locally straight (i.e. not changing orientation with position). Earlier such (straight) regions were excluded from the patterns considered in the analysis to avoid higher order evaluations of the parameter H. Regions where the Hessian is zero are known to correspond to catastrophes in the focusing of light. Figure 4.4 shows a greyscale representation of the magnitude of the Hessian of the phase function shown in figure 4.1(b). A number of curves are visible with low values of $|H|$.

Figure 4.4.
The magnitude of the Hessian of the phase. Greyscale encoding means blacks represents 0 and white represents peak value. The magnitude has been set to zero in the outer region where the fringe amplitude is insignificant.

In the book by Nye[19] his equation (2.10) corresponds directly with the condition in equation (4.48) above. The main difficulty with catastrophes is the singularity in the Fourier amplitude so introduced. Incorporation of catastrophes (also equivalent to the merging of multiple stationary points) in our stationary phase analysis is possible but may be expected to make many of the important derivations lengthy and complicated. In this chapter only fringe patterns with isolated (interior) stationary points are considered. This then implies that there is always a frequency shift (due to the orientation phase gradient) for the patterns under consideration. The frequency shift means that there is a frequency component at $\left(u_s - \Delta u_s, v_s - \Delta v_s\right)$ with a phase $k\left[\psi\left(\breve{x}_n, \breve{y}_n\right) - \beta\left(\breve{x}_n, \breve{y}_n\right)\right]$. The frequency shift can be expected to introduce a discrepancy between the ideal spiral Fourier phase and the actual phase contribution calculated via stationary phase. Comparing this to a kth order spiral phase in the Fourier domain is possible by estimating the rotation $\Delta\phi$ caused by the frequency shift:

$$\tan\left(\phi + \Delta\phi\right) = \tan\left(\frac{v_s - \Delta v_s}{u_s - \Delta u_s,}\right). \tag{4.49}$$

The error propagation property of the arctangent[20] is used to find a small angle error approximation:

$$\Delta\phi \simeq \frac{u_s \Delta v_s - v_s \Delta u_s}{u_s^2 + v_s^2}, \left(\Delta u_s\right)^2 \ll u_s^2 + v_s^2, \left(\Delta v_s\right)^2 \ll u_s^2 + v_s^2. \tag{4.50}$$

Using the values above for these parameters results in

$$\Delta\phi \simeq \frac{\psi_{1,0}^2\psi_{0,2} + \psi_{0,1}^2\psi_{2,0} - 2\psi_{1,0}\psi_{0,1}\psi_{1,1}}{\left(\psi_{1,0}^2 + \psi_{0,1}^2\right)^2} = \frac{\psi_{1,0}^2\psi_{0,2} + \psi_{0,1}^2\psi_{2,0} - 2\psi_{1,0}\psi_{0,1}\psi_{1,1}}{\left(\psi_{1,0}^2 + \psi_{0,1}^2\right)^{3/2}} \frac{1}{\left(\psi_{1,0}^2 + \psi_{0,1}^2\right)^{1/2}} \tag{4.51}$$

The above formula may be recognised as the curvature of a two-dimensional function ψ (see Granlund[21], page 361, for example) divided by the magnitude of the gradient. Experimentally[4] the errors apparently follow the relative curvature during testing of the spiral phase algorithm. The above result indicates that the proportionality constant is simply one. Figure 4.5(a) shows a greyscale representation of the relative curvature function in equation (4.51).

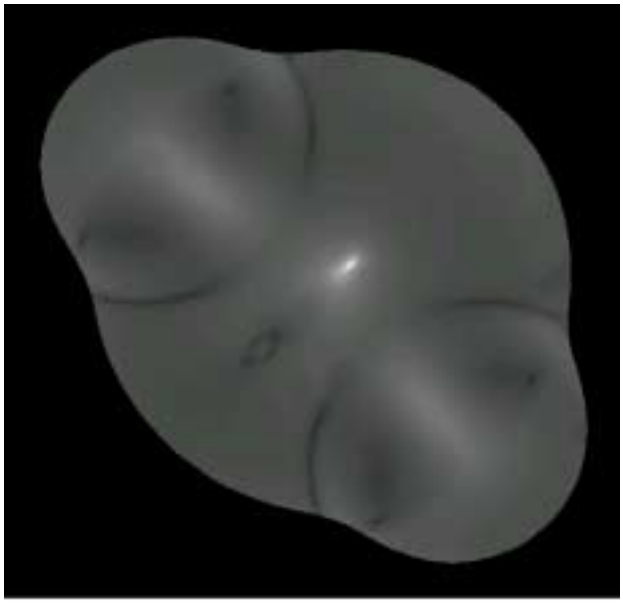

Figure 4.5(a).
Sixth root of the magnitude of the relative curvature of the phase. Greyscale encoding means blacks represents 0 and white represents peak value. The magnitude has been set to zero in the outer region where the fringe amplitude is insignificant. The sixth root is chosen to emphasize certain features.

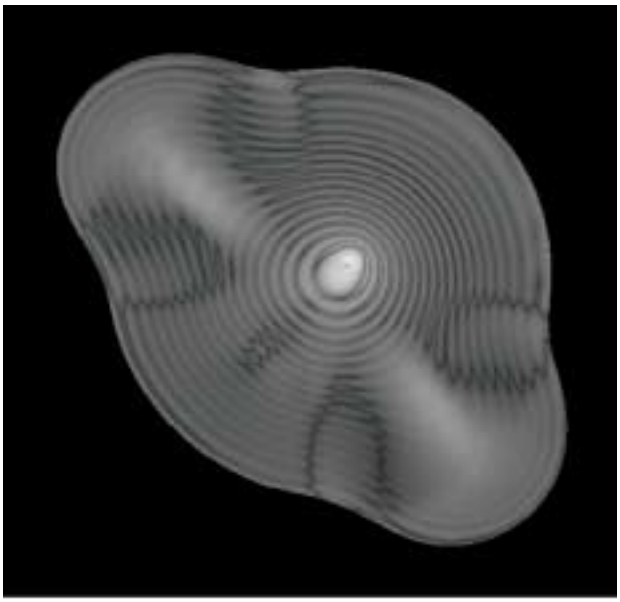

Figure 4.5 (b).
Sixth root of the magnitude of actual error in the phase derived using the vortex operator on the fringe pattern of figure 4.1(a). Greyscale as in 4.5(a).

Figure 4.5(b) is a greyscale representation of the actual phase error arising from vortex operator demodulation. Apart from the residual fringe structure in figure 4.5(b), the two figures are broadly consistent, especially regarding the location of extrema.

The frequency shifting gives rise to a phase error when compared to the Fourier spiral phase. Another effect is related to the amplitude change due to the Hessian at the critical point is given by

$$\begin{aligned}\breve{H}\left(\breve{x}_n,\breve{y}_n\right) &= \breve{\Psi}_{0,2}\left(\breve{x}_n,\breve{y}_n\right)\breve{\Psi}_{2,0}\left(\breve{x}_n,\breve{y}_n\right)-\breve{\Psi}_{1,1}^2\left(\breve{x}_n,\breve{y}_n\right)\\ &= \left(\psi_{0,2}-\beta_{0,2}\right)\left(\psi_{2,0}-\beta_{2,0}\right)-\left(\psi_{1,1}-\beta_{1,1}\right)^2. \\ &= H\left(\breve{x}_n,\breve{y}_n\right)+\left(\beta_{2,0}\beta_{0,2}-\beta_{1,1}^2\right)-\left(\psi_{0,2}\beta_{2,0}+\psi_{2,0}\beta_{0,2}-2\psi_{1,1}\beta_{1,1}\right)\end{aligned} \tag{4.52}$$

So, in general, the amplitude of $\breve{P}_k\left(\breve{u}_s,\breve{v}_s\right)_n$ is different to the first stationary phase expansion by an amount that depends upon the second order derivatives of both the underlying phase and the orientational phase. This is broadly consistent with initial

simulations of 2-D demodulation using the spiral phase quadrature operator.[4] The relative error in the local Hessian is as follows:

$$\frac{\Delta H}{H} = \frac{\left(\beta_{2,0}\beta_{0,2} - \beta_{1,1}^2\right) - \left(\psi_{0,2}\beta_{2,0} + \psi_{2,0}\beta_{0,2} - 2\psi_{1,1}\beta_{1,1}\right)}{\psi_{2,0}\psi_{0,2} - \psi_{1,1}^2}. \tag{4.53}$$

There are a variety of situations where the relative error is zero, the simplest being when the orientation is locally linear ($\beta_{2,0} = \beta_{0,2} = \beta_{1,1} = 0$). The detailed analysis of the amplitude error propagation will not be pursued further in this preliminary investigation. Figure 4.6 shows a greyscale representation of the actual amplitude error calculated for the vortex operator demodulation. The main errors are constrained to the centre of the fringe pattern. The centre of the fringe pattern also corresponds to a region where the orientation components (defined in equation (4.47)) are singular ($\psi_{1,0}^2 + \psi_{0,1}^2 = 0$).

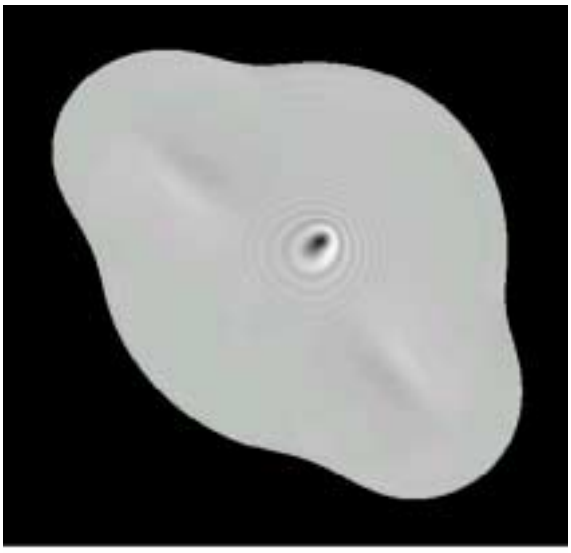

Figure 4.6.
Relative magnitude of the vortex operator derived magnitude. Greyscale encoding means blacks represents 0 and white represents peak value. Central region values vary from 0.16 to 1.30 with most regions near the ideal 1.00.

4.8 Conclusion

The validity of the intuitively inspired spiral phase quadrature transform has been confirmed using the method of stationary phase. I have shown that taking a quadrature fringe pattern and multiplying it by an orientational phase pattern followed by Fourier transformation gives the same as Fourier transforming a fringe pattern and then multiplying by a spiral phase factor. Using an alternative formulation of the stationary phase method I have shown how phase errors arise when the radius of curvature of the fringe pattern is small (curvature large) compared to the fringe spacing. Amplitude errors in the spiral phase transform are related to more complicated combinations of second and higher order derivatives of the phase function underlying the fringe pattern. A theoretical basis for further developments in direct, two-dimensional fringe demodulation and analysis has been established.

4.9 Connections

4.9.1 The analytic signal, the envelope, and the instantaneous frequency

The concepts of analytic signal, the envelope and the instantaneous frequency (discussed initially in chapter 2) can all be extended to two dimensions using the vortex transform. Extensions to three or more dimensions are straightforward but require the Riesz transform and hypercomplex numbers (or vectors).[4]

4.9.2 The multidimensional energy operator

The energy operator has been extended from one dimension [25] but the formalism is limited to positive values for each component which limits the concept

to orientations within one orthant (or quadrant in 2-D), which may be more limiting than is necessary. Using the spiral phase transform as a template, an alternative definition of the 2-D energy operator is possible. A 2-D form of the five-sample adaptive (FSA) algorithm has not yet been found.

4.9.3 The Radon transform, the complex gradient and the spiral phase transform

These 2-D concepts are easily related by their Fourier transform properties. In the Fourier domain all these operators are multiplicative. The dual R^* (also the adjoint) of the Radon transform when applied to the Radon transform R has a particularly simple interpretation as a convolution[26]

$$\mathrm{R}^*\,\mathrm{R}\{f(x,y)\} = f(x,y) * \left(\frac{1}{r}\right) \rightleftharpoons \frac{F(u,v)}{q}.$$

The complex gradient operator (Cauchy operator) C is defined by

$$\mathrm{C}\{f(x,y)\} = \frac{1}{2}\left(\frac{\partial}{\partial x} + i\frac{\partial}{\partial y}\right) f(x,y) \rightleftharpoons -\pi i(u+iv)F(u,v) = -\pi i q \exp(i\phi) F(u,v)$$

The spiral phase transform (denoted by \$ here) can also be represented as a convolution

$$\$\{f(x,y)\} = f(x,y) * \left(-i\frac{\exp(i\theta)}{r^2}\right) \rightleftharpoons \exp(i\phi) F(u,v).$$

The resulting inter-relations are

$$\mathrm{R}^{*}\,\mathrm{R}\left\{\mathrm{C}\left\{f(x,y)\right\}\right\}=\mathrm{C}\left\{\mathrm{R}^{*}\,\mathrm{R}\left\{f(x,y)\right\}\right\}=-\pi i\$\left\{f(x,y)\right\}.$$

Many of the crucial properties of the phase space functions like the ambiguity function and the Wigner distribution function are related by projections such as the Radon transform. A connection with Chapter 3 is that the integral in equation (3.14) can be viewed as a projection along a circular arc. The above relations can be easily inverted to reveal the original function from its Radon-Radon dual transform:

$$\frac{\$^{-1}\left\{\mathrm{C}\left\{\mathrm{R}^{*}\,\mathrm{R}\left\{f(x,y)\right\}\right\}\right\}}{-\pi i}=f(x,y).$$

Because of these properties the spiral phase transform may be expected to have applications in phase space analysis of signals.

4.9.4 Nth order spiral phase operator and the inverse operator

The inverse of the spiral phase operator is just a spiral operator with a reversed spiral. Exact inversion isn't always possible because, like the 1-D Hilbert transform, it loses the DC component. More generally the extension to the n^{th} order is simply

$$\$^{n}\left\{f(x,y)\right\}=\mathrm{F}^{-1}\left\{e^{in\phi}\,\mathrm{F}\left\{f(x,y)\right\}\right\},$$

but the application and interpretation of such higher order operators is still under consideration.

4.10 Appendix: Practical Aspects of the Fringe Orientational Factor

The correct functioning of the vortex transform depends upon the correct definition and evaluation of the orientation angle $\beta(x,y)$. For a complex function the definition follows simply from the phase gradient. For real fringes there is always an ambiguity due to a loss in some sign information as shown by:

$$\cos(\psi) = \cos(-\psi). \tag{4A.1}$$

This sign ambiguity is well known in interferometry (i.e. see Kreis[22]). There is a significant advantage which emerges from the vortex transformation approach to fringe demodulation. The advantage is that the ambiguity resides purely in the choice of sign for the fringe orientation because the fundamental quadrature operation has been performed already by the spiral phase Fourier multiplier. Now the underlying assumption in this work is that we are dealing with (open or closed) fringe patterns with smooth and infinitely differentiable amplitude and phase parameters. This means that the fringe orientation is everywhere smooth and differentiable, except at special points where the phase gradient is identically zero and the orientation is undefined. Interestingly these points give rise to spiral phase singularities in the orientation phase factor $\exp(-i\beta)$, evoking the concept of ever decreasing spirals! Singularities in the orientation can only occur at points where $\nabla\psi = 0$, points that have a stationary phase Fourier component at zero frequency ($u_s = v_s = 0$) which is the one frequency where the spiral phase factor is effectively undefined. (Considering its value as the average of its limiting value as the origin is approached from different

directions, then the modulus is zero and the phase is undefined). In general these singular points of orientation will have problematic expansions in terms of conventional power series.

Another problem with evaluation of the fringe orientation is the effect of amplitude modulation on the phase gradient estimate. In general the amplitude modulation is unknown *a priori*, leading to a signal gradient ∇f which deviates from the phase gradient $\nabla\psi$:

$$\nabla f = \cos\psi\nabla b - b\sin\psi\nabla\psi\,. \tag{4A.2}$$

The error in the estimated orientation is then ε, where

$$\tan\beta_{est} = \tan\left(\beta+\varepsilon\right) = \frac{f_{0,1}}{f_{1,0}} = \frac{\psi_{0,1}b\sin\psi - b_{0,1}\cos\psi}{\psi_{1,0}b\sin\psi - b_{1,0}\cos\psi}\,. \tag{4A.3}$$

And it can be shown that

$$\tan\varepsilon = \frac{\left(\psi_{0,1}b_{1,0} - \psi_{1,0}b_{0,1}\right)\cos\psi}{\left(\psi_{0,1}^2 + \psi_{1,0}^2\right)b\sin\psi - \left(\psi_{1,0}b_{10} + \psi_{0,1}b_{0,1}\right)\cos\psi} \tag{4A.4}$$

which means that the orientation error is always zero at zero crossings of f (i.e. $\cos\psi = 0$), and at regions where the amplitude gradient either is zero, or is in the same direction (modulo π) as the phase gradient:

$$\frac{b_{0,1}}{b_{1,0}} = \frac{\psi_{0,1}}{\psi_{1,0}} \equiv \tan\beta\,. \tag{4A.5}$$

In other situations the error is non-zero.

Finally a few observations about practical schemes for estimating the orientation modulo 2π, as required by our spiral phase demodulation method. The first point to note is that simple gradient based schemes suffer from sign flips that occur in every period of a real fringe pattern. Given the complex fringe pattern, then the gradient can be calculated

$$\nabla\{\exp(i\psi)\} = \exp(i\psi)\nabla\psi . \tag{4A.6}$$

Given the cosine component only, then

$$\nabla\{\cos\psi\} = -\sin\psi\nabla\psi \ . \tag{4A.7}$$

The actual angle can be obtained from an arctangent of the gradient components:

$$\beta = \arctan\left(\frac{-\psi_{0,1}\sin\psi}{-\psi_{1,0}\sin\psi}\right). \tag{4A.8}$$

The problem here is that the sine components do not simply cancel out because the arctangent quadrants flip polarity in synchrony with the sine polarity. The same problem arises if spiral phase transform itself is used to estimate the orientation:

$$i\exp(-i\beta)b\sin\psi \sim \mathrm{F}^{-1}\{\exp(i\phi)\mathrm{F}\{b\cos\psi\}\} \tag{4A.9}$$

$$\arg\left\{i\exp(-i\beta)b\sin\psi\right\} = \arctan\left\{\frac{\cos\beta\sin\psi}{\sin\beta\sin\psi}\right\} \qquad (4A.10)$$

and the sine multiplier introduces an ambiguity in the tangent quadrants again. There is also another (related) insidious problem with gradient based orientation estimation which occurs when the sine component approaches zero ($\sin\psi \to 0 \Leftrightarrow \cos\psi \to \text{extremum}$) and the practical orientation estimate becomes very noise sensitive. Yu and Andresen[23] considered a median filtering solution to the problem of estimating orientation maps in 1994. Although practical aspects of noise analysis are not considered in this chapter, it is clear that an orientation estimate which is independent of the value of $\sin\psi$ is desirable. Second derivatives of the fringe pattern could be used which are related to the value of $\cos\psi$. By combining both $\sin\psi$ and $\cos\psi$ factors it is possible to obtain uniform (i.e. independent of ψ) estimates of the orientation. The details are not considered here - as the subject warrants a paper on its own – except to note that methods based upon the energy operator,[24, 25] or tensor analysis[21] are recommended. In either case the estimate of the orientation always occurs in a quadratic form i.e. $\exp(2i\beta)$. This is really just another incarnation of the sign ambiguity:

$$\exp(i\beta)_{estimate} = \pm\sqrt{\exp(2i\beta)}\,. \qquad (4A.11)$$

Perhaps the easiest way (whilst not forgetting that there are other methods) to obtain the final result required (orientation estimate modulo 2π) is to unwrap

2β modulo 4π and then halve it. Remember that the unwrapping is relatively straightforward because the underlying assumption is for smoothly varying phase, hence smoothly varying orientation (except at the centres of closed curves as discussed earlier). Figure 4.3(a) shows an orientation phase map ($+\sqrt{\exp(2i\beta)}$) which has not been unwrapped versus figure 4.3(b) which shows a correctly unwrapped ($\exp(i\beta)$) map.

4.11 Acknowledgments

I wish to thank Don Bone and Michael Oldfield who have encouraged my unraveling of the spiral phase transform.

4.12 References and notes

1 R. Penrose, "The topology of ridge systems", Ann. Hum. Genet.,Lond. **42**, 435-444, (1979).

2 M. Kass, and A. Witkin, "Analyzing oriented patterns", Computer vision, graphics, and image processing **37**, 362-385, (1987).

3 C. F. Shu, and R. C. Jain, "Direct Estimation and Error Analysis For Oriented Patterns", CVGIP-Image Understanding **58**, (3), 383-398, (1993).

4 K. G. Larkin, D. Bone, and M. A. Oldfield, "Natural demodulation of two-dimensional fringe patterns: I. General background to the spiral phase quadrature transform.", Accepted for publication in the Journal of the Optical Society of America, A, (to appear circa July 2001).

5 Z. Jaroszewicz, A. Kolodziejczyk, D. Mouriz, and S. Bara, "Analytic design of computer-generated Fourier-transform holograms for plane curves reconstruction.", J. Opt. Soc. Am., A **8**, (3), 559-565, (1991).

6 M. A. Stuff, and J. N. Cederquist, "Coordinate transformations realizable with multiple holographic optical elements", J. Opt. Soc. Am., A **7**, (6), 977-981, (1990).

7 There are a number of ways to remove the offset. Low pass filtering is the simplest but often not the best method. In situations with multiple phase-shifted interferograms the difference of any two frames will have the offset nullified. Adaptive filtering methods can also provide more accurate offset removal.

8 A. H. Nuttall, "On the quadrature approximation to the Hilbert transform of modulated signals", IEEE Proceedings **54**, 1458-1459, (1966).

9 M. Takeda, H. Ina, and S. Kobayashi, "Fourier-transform method of fringe-pattern analysis for computer-based topography and interferometry", J. Opt. Soc. Am. **72**, (1), 156-160, (1982).

10 D. J. Bone, H.-A. Bachor, and R. J. Sandeman, "Fringe-pattern analysis using a 2-D Fourier transform", App. Opt. **25**, (10), 1653-1660, (1986).

11 J. L. Marroquin, J. E. Figueroa, and M. Servin, "Robust Quadrature Filters", Journal of the Optical Society of America A-Optics & Image Science **14**, (4), 779-791, (1997).

12 N. Bleistein, and R. A. Handelsman, Asymptotic expansion of integrals, Reprint, Dover Books Inc, New York, 1975.

13 We shall refrain from calling this function the 2D analytic signal because there are several conflicting definitions of analyticity in multiple dimensions including the next reference.

14 M. A. Fiddy, "The role of analyticity in image recovery", Image recovery: theory and application, ed. Stark, H. (Florida: Academic Press, 1987).

15 J. J. Stamnes, Waves in focal regions, Adam Hilger, Bristol, 1986.

16 The Gaussian curvature C at a critical point (zero gradient) is equal to the Hessian.

$$C = \frac{\psi_{2,0}\psi_{0,2} - \psi_{1,1}^2}{\left(1 + \psi_{1,0}^2 + \psi_{0,1}^2\right)^{3/2}} = \frac{H}{\left(1 + \psi_{1,0}^2 + \psi_{0,1}^2\right)^{3/2}}$$

$$\psi_{1,0} = \psi_{0,1} = 0 \Rightarrow C = H$$

17 A. Papoulis, Systems and transforms with applications in optics, McGraw-Hill, New York, 1968.

18 A zero gradient of the orientation implies a zero Hessian. The converse is not true, as there are surfaces, such as the cone, with zero Hessian and non-zero orientation gradient.

19 J. F. Nye, Natural focusing and the fine structure of light, Institute of Physics Publishing, Bristol, 1999.

20 K. G. Larkin, and B. F. Oreb, "Propagation of errors in different phase-shifting algorithms: a special property of the arctangent function," SPIE Proc. Vol **1755**, 219-227, (1992),.

21 G. H. Granlund, and H. Knutsson, Signal processing for computer vision, Kluwer, Dordrecht, Netherlands, 1995.

22 T. Kreis, Holographic interferometry. Principles and methods, 1, Akademie Verlag GmbH, Berlin, 1996.

23 Q. Yu, and K. Andresen, "Fringe-orientation maps and fringe skeleton extraction by the two-dimensional derivative-sign binary-fringe method", App. Opt. **33**, (29), 6873-6878, (1994).

24 J. F. Kaiser, "On a simple algorithm to calculate the 'energy' of a signal," Proc IEEE Int. Conf. Acoust. Speech, Signal Processing, Albuquerque, NM, (1990), 381-384.

25 P. Maragos, A. C. Bovik, and T. F. Quatieri, "A multidimensional energy operator for image processing," SPIE Proc. **1818**, 177-186 (1992).

26 R. S. Strichartz, "Radon inversion - variations on a theme", Amer. Math. Monthly **89**, (6), 377-384, (1982).